Molecular Biology of the Cell
Vol. 16, 4918–4930, October 2005

Control of Golgi Morphology and Function by Sed5 t-SNARE Phosphorylation

Adina Weinberger,* Faustin Kamena,† Rachel Kama,* Anne Spang,† and Jeffrey E. Gerst*

*Department of Molecular Genetics, Weizmann Institute of Science, Rehovot 76100, Israel; and †Friedrich Miescher Laboratory, Max Planck Society, D-72076 Tuebingen, Germany

Submitted February 7, 2005; Revised July 25, 2005; Accepted August 2, 2005
Monitoring Editor: Howard Riezman

Previously, we demonstrated that the phosphorylation of t-SNAREs by protein kinase A (PKA) affects their ability to participate in SNARE complexes and to confer endocytosis and exocytosis in yeast. Here, we show that the presumed phosphorylation of a conserved membrane-proximal PKA consensus site (serine-317) in the Sed5 t-SNARE regulates endoplasmic reticulum (ER)-Golgi transport, as well as Golgi morphology. Sed5 is a phosphoprotein, and both alanine and aspartate substitutions in serine-317 directly affect intracellular protein trafficking. The aspartate substitution results in elaboration of the ER, defects in Golgi-ER retrograde transport, an accumulation of small transport vesicles, and the inhibition of growth of most cell types. In contrast, the alanine substitution has no deleterious effects upon transport and growth, but results in ordering of the Golgi into a structure reminiscent of mammalian apparatus. This structure seems to require the recycling of Sed5, because it was found not to occur in *sec21-2* cells that are defective in retrograde transport. Thus, a cycle of Sed5 phosphorylation and dephosphorylation is required for normal t-SNARE function and may choreograph Golgi ordering and dispersal.

INTRODUCTION

The secretory pathway in eukaryotes consists of distinct membrane-bound intracellular compartments that transfer proteins and lipids in bulk from one to the other. This occurs via transport structures that undergo fusion with subsequent compartments. Because these compartments are in a constant state of flux, due to the continuous exchange of membrane and protein, obligate protein sorting and retrieval mechanisms have evolved to maintain organelle identity and integrity. Moreover, there is a specific need for recreating intact and functional organelles after mitosis, via organelle inheritance and/or biogenesis. The Golgi apparatus consists of well-defined subcompartments (cisternae) arranged in an ordered structure in higher eukaryotes, called the Golgi stack, which displays an asymmetric distribution of specific processing enzymes (reviewed in Farquhar and Palade, 1998). Cargo molecules traverse the stack via the process of cisternal maturation, which involves the retrograde flow of enzymes and transport factors back to earlier compartments while allowing the cargo to proceed (reviewed in Pelham, 1998; Pelham and Rothman, 2000). This results in steady-state distribution of the protein processing and delivery factors while allowing cargo to advance and eventually exit the Golgi via transport vesicles.

The fusion of membranes along the secretory pathway involves SNAREs, which comprise three main families of conserved membrane-associated proteins (the VAMP/synaptobrevin, syntaxin, and SNAP-25/light chain families) that mediate vesicle docking and fusion (reviewed in Chen and Scheller, 2001). Conventionally, these families fall into two categories, the v-SNAREs that reside on vesicles and t-SNAREs that reside on the acceptor compartments. Both v- and t-SNAREs assemble into a four-helix bundle that bridges apposed membranes and leads to membrane fusion (reviewed in Chen and Scheller, 2001). The v-SNARE contributes one α-helix to the SNARE complex, whereas three are contributed by the t-SNAREs. Notably, every intracellular trafficking step has one syntaxin t-SNARE that serves as an essential element of the fusion complex. In yeast, the syntaxin family member, Sed5, plays an essential role in protein transport from the endoplasmic reticulum (ER) to the Golgi as well as intra-Golgi transport (Hardwick and Pelham, 1992, Nichols and Pelham, 1998). Sed5 forms functional SNARE complexes with Sec22, Bet1, and Bos1 (Sogaard *et al*., 1994; Parlati *et al*., 2002) to mediate ER–Golgi transport and with other SNAREs, such as Sft1, Ykt6, Gos1, and Vti1 to mediate intra-Golgi and endosome-Golgi transport (reviewed by Pelham, 1999). Attempts to systematically define the number of possible Sed5-containing SNARE complexes revealed that it is promiscuous and forms numerous complexes in vitro (Tsui *et al*., 2001); however, only two have been shown to be functional using an in vitro fusion assay (Parlati *et al*., 2002). Nevertheless, the large number of complexes that Sed5 forms in vitro may reflect its importance in the maintenance of Golgi structure and function.

Sed5 localizes to the *cis*-Golgi (Hardwick and Pelham 1992) and cycles through the ER (Wooding and Pelham, 1998). However, it is not known how Sed5 is retained at steady state in the Golgi and what physiological purpose is served by recycling. In an attempt to define its retention signal, mutations were made in the transmembrane domain (TMD), which is known to play a role in the retention of other SNAREs (Lewis *et al*., 2000). However, the Sed5 local-

This article was published online ahead of print in *MBC in Press* (http://www.molbiolcell.org/cgi/doi/10.1091/mbc.E05–02–0101) on August 10, 2005.

Address correspondence to: Jeffrey E. Gerst (jeffrey.gerst@weizmann.ac.il).

Table 1. Yeast strains

Name	Genotype	Source
SP1	*MAT***a** *ura3 leu2 trp1 ade8 his3 can1*	M. Wigler
W303-1b	*MAT***a** *ura3 leu2 trp1 ade2 his3 lys2 can1*	J. Hirsch
*ise1*Δ	*MAT***a** *his3Δ1 leu2Δ0 met15Δ0 ura3Δ0 ise1::kanMX4*	EUROSCARF
*grh1*Δ	*MAT***a** *his3Δ1 leu2Δ0 met15Δ0 ura3Δ0 grh1::kanMX4*	EUROSCARF
SP1-SEC7RFP	*MAT***a** *ura3 leu2 ade8 can1 his3 trp1::TRP1::TPI1-DsRed-SEC7*	J. Gerst
MLY101	*MAT***a**, *trp1–1 ufe1::TRP1 his3-200 leu2-3, 112 ura3-52 ufe1::TRP1* pUT1 *(CEN6 LEU2 ufe1-1)*	M. Lewis
CBY265	*MAT***a** *trp1 ura3 leu2 lys2 sed5-1*	C. Barlowe
*sed5*Δ	*MAT***a** *ura3::GAL-SED5 sed5::LEU2 trp1-1*	D. Banfield
NY1217	*MAT***a** *ura3-52 leu2-3, 112 sec18-1*	P. Novick
RSY1309	*MAT***a** *ura3-52 leu2-3, 112 lys2-801 suc2-9 sec21-2*	A. Spang
RSY324	*MAT***a** *ura3-52 sec22-2*	R. Schekman
RSY641	*MAT***a** *ura3-52 leu2-3, 112 sec23-2*	R. Schekman
RKY1	*MAT***a** *ura3 leu2 trp1 ade8 sed5::GFP-SED5::his5+ can1*	This study
RKY2	*MAT***a** *ura3 leu2 trp1 ade8 sed5::GFP-SED5^{A317}::his5+ can1*	This study
RKY3	*MAT***a** *ura3 leu2 trp1 ade8 sed5::GFP-SED5^{D317}::his5+ can1*	This study

EUROSCARF, European *Saccharoymces cerevisiae* archive for functional analysis.

ization signal is only partially determined by its TMD (Banfield *et al*., 1994), and thus an additional localization/retention mechanism exists. In addition to regulating transport to the Golgi, Sed5 and its orthologues play an important role in Golgi maintenance and structure. The loss of Sed5 function is characterized by the accumulation of small transport vesicles and an elaboration of ER membranes concomitant with a decrease in protein transport and cell viability (Hardwick and Pelham, 1992). ER expansion is indicative of a block in the exit of proteins from the ER, which may result from an inhibition in retrograde transport from the Golgi. Interestingly, the overproduction of Sed5 is also inhibitory to cell growth, resulting in the accumulation of intracellular membranes and secretion of an ER resident protein (Hardwick and Pelham, 1992). Moreover, Sed5 orthologues have prominent effects upon Golgi structure. For example, the overproduction of *Drosophila* Sed5 results in the loss of Golgi stacks in COS cells (Banfield *et al*., 1994), whereas that of the NH_2-terminal sequence of mammalian Syntaxin-5 disrupts the Golgi in Vero cells (Yamaguchi *et al*., 2002).

We have demonstrated a role for t-SNARE phosphorylation in the regulation of exocytosis and endocytosis in yeast. Dephosphorylation of the Sso and Tlg t-SNAREs was found to enhance SNARE assembly and to restore transport in certain secretory mutants (Marash and Gerst, 2001; Gurunathan *et al*., 2002; Weinberger and Gerst, 2004). In our studies on the role of signaling cascades in the control of membrane transport, we have now examined whether Sed5 is controlled by phosphorylation. We found that Sed5 is a phosphoprotein that harbors a highly conserved PKA phosphorylation site proximal to the TMD. Amino acid substitutions in this site, serine-317, have dramatic effects upon Golgi morphology and function. Expression of pseudophosphorylated Sed5, shown using an aspartate substitution, results in the accumulation of ER and transport vesicles and an inhibition in cell growth. In contrast, expression of a nonphosphorylated form of Sed5, using an alanine substitution, results in the accumulation of an ordered Golgi atypical to *Saccharomyces cerevisiae*. This structure was absent in *sec21-2* cells, which are defective in Golgi-ER and intra-Golgi retrograde transport, suggesting a role for Sed5 recycling in its ability to induce ordered structures. Supportive of this idea, we found that the nonphosphorylated, but not pseudophosphorylated, form of Sed5 readily entered into transport COPI vesicles. These results suggest that Sed5 phosphorylation and dephosphorylation may play a crucial role in Golgi function and structure. In particular, it may allow for the Golgi to cycle between ordered and dispersed states, the latter being important for Golgi inheritance during mitosis (Shorter and Warren, 2002).

MATERIALS AND METHODS

Growth Tests

Yeast were grown in standard amino acid-rich medium (YPD) or selective synthetic media (SC).

Drop Tests. Cells were grown to log phase in liquid selective medium. Next, cells were diluted to 10^6 cells/ml, followed by five serial dilutions of 10-fold each. Aliquots of the dilutions were applied as drops onto solid media, which were then incubated at various temperatures.

Yeast Strains

Strains are listed in Table 1.

Plasmids

Constructs for SED5 Expression. *SED5* was amplified by PCR using genomic DNA as a template and primers encoding *Sal*I and *Sac*I sites at the 5′ and 3′ ends, respectively. The *Sal*I-*Sac*I fragment was inserted in-frame and downstream to the hemagglutinin (HA) epitope encoded by vector pAD54 (2μ, *LEU2*), to yield pADH-HASED5. *SED5* is under the control of the constitutive *ADH1* promoter. Next, a *Bam*HI fragment containing *ADH1-HASED5* was excised from pADH-HASED5 and cloned into plasmids pRS315 (*CEN; LEU2*) to yield pLADH-HASED5, pSE358 (*CEN; TRP1*) to yield pTADH-HASED5, and pRS426 (2μ, *URA3*) to yield pADHU-HASED5. Point mutations were made in *SED5* to create the alanine-317 and asparate-317 substitutions, by PCR-based site-directed mutagenesis with *Pfu*I polymerase (Stratagene, La-Jolla, CA). Multicopy plasmids bearing either *LEU2* or *URA3* and single-copy plasmids bearing either *LEU2* or *TRP1*, all of which express *SED5*, *SED5^{S317A}*, or *SED5^{S317D}* were created. A gene encoding green fluorescent protein (GFP) was introduced in-frame and upstream to *SED5* by subcloning a *Sal*I *GFP* fragment into the *Sal*I site of the *LEU2* multicopy *SED5* plasmids. This created *HA-GFP* fusions with *SED5*, *SED5^{S317A}*, or *SED5^{S317D}*. Next, the gene fusions were excised as *Bam*HI fragments and cloned into the *Bam*HI site of pRS315 to yield the same fusions in single-copy plasmids. Constructs for the integration of *HA-GFP* tagged *SED5*, *SED5^{S317A}*, or *SED5^{S317D}* at the native *SED5* locus were created by subcloning into plasmid pFA6a-His3MX6 (Longtine *et al*., 1998), which encodes a PCR amplification module for integration at target genes. *Hind*III and *Bam*HI fragments bearing the different *GFP*-tagged forms of *SED5* were subcloned from the pAD54 plasmids into plasmid pFA6a-His3MX6 via the *Hind*III and *Bam*HI sites. After verification by sequencing, plasmids were amplified using a 62-bp forward chimeric oligonucleotide corresponding to the 5′ untranslated region of *SED5* and downstream *HA-GFP*, and a 60-bp reverse oligonucleotide corresponding to the promoter

region of the *Schizosaccharomyces pombe his5+* gene and 3′ untranslated region of *SED5*. PCR amplified fragments were used to transform SP1 wild-type cells and were selected for on medium lacking histidine. Integration at the *SED5* locus was verified by PCR. A plasmid expressing Sec22-myc-α, pWB-GalAα, was provided by H-D. Schmidt (University of Gottingen, Germany).

Metabolic Labeling In Vivo

Protein Phosphorylation In Vivo. Proteins were metabolically labeled in vivo either with [^{32}P]orthophosphate or [^{33}P]orthophosphate (0.25 and 0.65 mCi/10 O.D.$_{600}$ U, respectively; GE Healthcare, Piscataway, NJ), essentially as described previously (Marash and Gerst, 2001).

Pulse-Chase Analysis. Intracellular protein processing was monitored by pulse-chase analysis using [^{35}S]methionine (GE Healthcare), as described previously (Couve *et al*., 1995).

Immunoprecipitation and Subcellular Fractionation

Immunoprecipitation. Coimmunoprecipitation from lysates was performed as described previously (Marash and Gerst, 2001). When performed in *sec18-1* lysates, the cell pellet was first washed with 10 mM NaN_3, and both 20 mM NaF and 1 mM *N*-ethylmaleimide were added to the lysis buffer. For the detection of phosphorylated Sed5 in Westerns or by autoradiography, the lysis buffer was supplemented with the following phosphatase inhibitors: 10 mM NaF, 20 mM NaPPi, 25 mM β-glycerophosphate, and 0.5 mM sodium vanadate. Proteins were detected in immunoblots by chemiluminescence.

Subcellular Fractionation. Yeast were subjected to subcellular fractionation, as described previously (Lustgarten and Gerst, 1999).

Antibodies

Monoclonal anti-HA antibodies (gift of M. Wigler, Cold Spring Harbor Laboratory, Cold Spring Harbor, NY) were used for both immunoprecipitation (IP) (1 μl) and detection (1:5000). Protein detection in blots was performed using monoclonal anti-c-myc (1:1000; Santa Cruz Biotechnology, Santa Cruz, CA) and polyclonal anti-phosphoserine (1:1000; Zymed Laboratories, South San Francisco, CA), anti-Sed5 (1:3000; gift of H. Pelham, MRC Laboratory for Molecular Biology, Cambridge, United Kingdom), anti-Bos1 (1:500), anti-Kar2 (1:3000; gifts of C. Barlowe, Dartmouth University, Hanover, NH), anti-Sec22 (1:3000; gift of S. Ferro-Novick, Yale University, New Haven, CT), anti-Vti1 (1:3000; gift of G. Fischer von Mollard, University of Gottingen); anti-Emp47 (1:3000; gift of H. Riezman, University of Geneva, Switzerland), anti-Dpm1 (1:1000; Molecular Probes, Eugene, OR), and anti-Mnn1 antibodies (1:2000; gift of S. Emr, University of San Diego, San Diego, CA). IP antibodies for pulse-chase experiments included anti-Gas1 (gift of H. Riezman) and anti-CPY (gift of S. Emr).

Microscopy

Confocal Microscopy. Cells were grown to log phase and concentrated to 1 O.D.$_{600}$ U/100 μl. Samples were mixed (1:1) with a cooled solution of 2.6% low melting point agarose in medium and plated on slides. GFP and red fluorescent protein (RFP; DsRed) fluorescence were visualized using a Radiance 2000 confocal system (Bio-Rad, Hercules, CA).

Immunofluorescence Microscopy. Cells were fixed and permeabilized for immunofluorescence, as described previously (Lustgarten and Gerst, 1999). HA-Sed5^{S317A} and HA-GFP-Sed5^{S317A} were labeled with affinity-purified anti-HA monoclonal antibodies and CY3-conjugated goat anti-mouse antibodies (Jackson ImmunoResearch Laboratories, West Grove, PA).

Electron Microscopy. Cells were concentrated by centrifugation, drawn into cellulose capillary tubes (200-μm inner diameter), and frozen in a Bal-Tec HPM010 HPF machine. For procedure A, cells were freeze-substituted in a Leica AFS device in anhydrous acetone containing 0.01% osmium tetroxide for 3 d at –90°C and then warmed to 0°C over 24 h. Samples were washed two times with ethanol and infiltrated for 5–7 d at room temperature (RT) in a series of increasing concentrations of LR-White in ethanol as follows: 5, 10, 30, 50, 60, 80%, and six exchanges of pure resin. After polymerization at 52°C, 60- to 80-nm sections were stained with uranyl acetate and lead citrate and examined in an FEI Tecnai T12 electron microscope at 120 kV. Alternatively, in procedure B, the frozen capillary tubes were freed from extraneous hexadecene under liquid nitrogen and freeze-substituted in 2% osmium tetroxide in anhydrous acetone at –90°C for 32 h, and at –60 and –30°C for 4 h at each step in a Balzers FSU010 freeze-substitution unit. After washing with acetone, samples were transferred into an acetone-Epon mixture at −30°C, infiltrated at RT in Epon, and polymerized at 60°C for 48 h. Ultrathin sections stained with uranyl acetate and lead citrate were viewed using a Philips CM10 electron microscope at 60 kV.

Golgi Budding Assay

In vitro Golgi budding was performed as described by Spang and Schekman (1998) with modifications. Enriched Golgi membranes were incubated with 0.1 mM GTP, coatomer (250 μg/ml), and Arf1 (80 μg/ml) for 30 min at 30°C in a volume of 200 μl. After chilling on ice, samples were loaded on top of a Ficoll-sucrose gradient consisting of 0.4 ml 60%(wt/wt) sucrose, 0.8 ml 7.5% (wt/wt) Ficoll, 1 ml of 5% Ficoll, 1 ml of 4% Ficoll, 1 ml of 3% Ficoll, 0.8 ml of 2% Ficoll in 15% sucrose, 20 mM HEPES, pH 6.8, and 5 mM $Mg(OAc)_2$. Vesicles were separated from the Golgi by centrifugation for 2 h at 35,000 rpm (SW55 rotor; Beckman Coulter, Fullerton, CA). Fractions (400 μl) were collected from the top of the gradient. Fractions 5–7 were pooled, mixed with an equal volume of 80% Nycodenz in 20 mM HEPES, pH 6.8, 150 mM KOAc, 5 mM $Mg(OAc)_2$ (B150), and overlaid with 600 μl of 30, 25, 20, and 15% and 400 μl of 10% Nycodenz in B150. The gradient was centrifuged for 16h at 40,000 rpm (SW55 rotor). Fractions (300 μl) were collected from the top, trichloroacetic acid precipitated, and analyzed in immunoblots.

RESULTS

Sed5 Is Phosphorylated In Vivo

PKA is involved in the regulation of the Sso and Tlg t-SNAREs, which confer exo- and endocytic transport in yeast, respectively (Marash and Gerst, 2001; Gurunathan *et al*., 2002). In the case of the Sso t-SNAREs, phosphorylation inhibits t-t SNARE assembly and recruits a SNARE regulatory protein, Vsm1, to the autoinhibitory domain of Sso (Marash and Gerst, 2001; Marash and Gerst, 2003). Correspondingly, activation of a ceramide-activated protein phosphatase (CAPP) reduces Vsm1 binding, restores t-t SNARE assembly, and confers exocytosis (Marash and Gerst, 2001; Marash and Gerst, 2003). Because phosphorylation and dephosphorylation play a significant role in t-SNARE regulation on the late secretory pathway, we examined whether ER–Golgi transport is controlled in a similar manner.

We examined whether temperature-sensitive mutations in SNAREs functioning in the early pathway might be rescued for growth at restrictive temperatures by the exogenous addition of C2-ceramide, a CAPP activator, to the medium. We found that a temperature-sensitive mutation in *SED5* (e.g., *sed5-1*), which encodes an essential Golgi t-SNARE of the syntaxin family, was partially rescued, whereas mutations in other SNAREs involved in ER–Golgi transport (i.e., *bos1-1*, *bet1-1*, and *sec22-1*) were either not affected or were inhibited (our unpublished data). Thus, Sed5 might be subject to regulation by phosphorylation.

We noticed two putative PKA phosphorylation sites present in Sed5: serine-8 and serine-317. The NH_2-terminal phosphorylation site (serine-8) resides proximal to the Habc domain (Figure 1A), which has a suggested regulatory role (Yamaguchi *et a*l., 2002). However, alignments of Sed5 orthologues revealed that only the COOH-terminal phosphorylation site (serine-317) is highly conserved from yeast to humans (Figure 1B). This site lies in the region directly downstream of the SNARE domain (residues 249–311) and proximal to the TMD (residues 325–339; Hardwick and Pelham, 1992) (Figure 1A).

To demonstrate whether Sed5 is a phosphoprotein, we first expressed a HA epitope-tagged form of Sed5 in yeast, performed in vivo labeling with [^{32}P]orthophosphate, and immunoprecipitated the protein. We examined Sed5 phosphorylation in vivo using a number of strains (e.g., WT, *sec18-1*, *bos1-1*). In particular, we found significant incorporation of labeled phosphate into HA-Sed5 in *bos1-1* cells, which bear a temperature-sensitive t-SNARE involved in ER–Golgi transport (Figure 1C). We could also demonstrate phosphorylation on serine residues using an antibody specific to phosphoserine (Figure 1D). In both experiments, a single band was observed corresponding to the molecular mass of HA-Sed5 (~42 kDa). Labeling of HA-Sed5 was

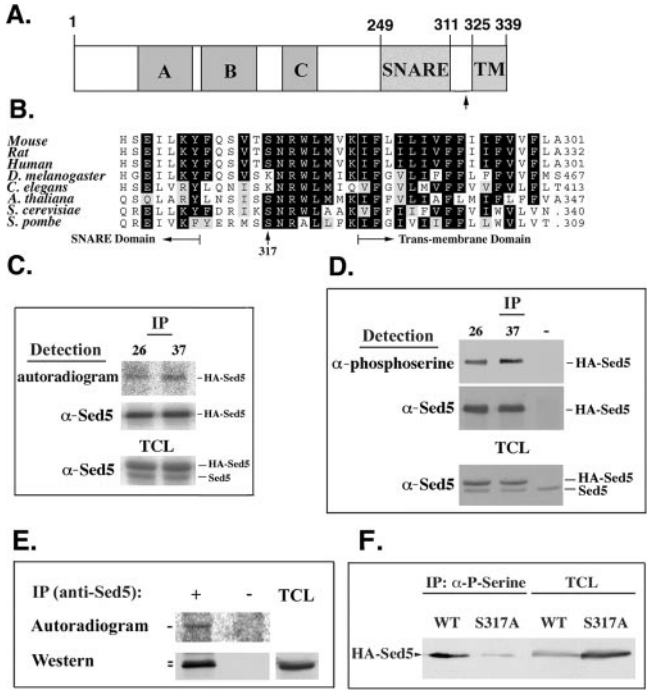

Figure 1. Sed5 is phosphorylated in *bos1-1* and wild-type cells. (A) Schematic of Sed5 structure. A, B, and C, α-helices of the putative autoinhibitory domain; *SNARE*, SNARE domain; *TM*, transmembrane domain. An arrow marks the location of serine-317. (B) Sequence alignment of *S. cerevisiae* Sed5 with Syntaxin-5 orthologues from other species. Only the last 36–37 residues of the alignment are presented. (C) HA-Sed5 is phosphorylated in *bos1-1* cells. HA-tagged Sed5 was expressed from a multicopy vector (pADH-HASED5) in *bos1-1* cells. Cells were harvested in log phase and labeled with [^{32}P]orthophosphate for 3 h, before being either shifted to 37°C for 15 min or maintained at 26°C. Cells were lysed in the presence of phosphatase inhibitors and HA-Sed5 was precipitated from lysates with anti-HA antibodies. Immunoprecipitated proteins were detected either in westerns with anti-Sed5 antibodies or by autoradiography (autoradiogram). Samples of the total cell extract (TCL) are shown beneath the IP results. (D) HA-Sed5 in *bos1-1* cells is recognized by anti-phosphoserine antibodies. Same as in C, except that unlabeled *bos1-1* cells were also transformed with a control plasmid (−). Immunoprecipitated proteins were detected in Westerns with either anti-Sed5 or anti-phosphoserine antibodies. (E) Endogenous Sed5 is phosphorylated in wild-type cells. Wild-type (SP1) cells were grown to log phase and labeled with [^{33}P]orthophosphate for 3 h before lysis and immunoprecipitation with (+) or without (−) anti-Sed5 antibodies (2 μl/10 O.D.$_{600}$ U). Immunoprecipitated proteins were detected in Westerns with anti-Sed5 antibodies or by autoradiography (autoradiogram). (F) Serine-317 is a bona fide phosphorylation site. Wild-type (SP1) cells overproducing HA-Sed5 or HA-Sed5^{S317A} (plasmids pADH-HASED5 or pADH-HASED5^{S317A}) were lysed and proteins precipitated using anti-phosphoserine antibodies (10 μl/10 O.D.$_{600}$ U/reaction) and detected with anti-HA antibodies in blots. TCL, total cell lysate (50 μg of protein).

found to increase somewhat (~30%; n = 3) in *bos1-1* cells shifted to the restrictive temperatures (37°C). This increase may result from the block in SNARE assembly, during which increased t-SNARE phosphorylation has been documented previously (Marash and Gerst, 2001).

Because exogenously expressed HA-Sed5 is phosphorylated in *bos1-1* cells, it was necessary to determine whether endogenous Sed5 also undergoes phosphorylation. We examined the phosphorylation of Sed5 expressed from its genomic locus in wild-type cells using [^{33}P]orthophosphate and immunoprecipitation with anti-Sed5 antibodies (Figure 1E). In Westerns detected with anti-Sed5, we observed two Sed5 bands that migrated closely (~39 and 41 kDa, respectively); however, autoradiography indicated that only the higher band incorporated the radiolabel (Figure 1E). Similar results might have been observed for HA-Sed5 (Figure 1, C and D), but its overexpression may have impeded resolution of the two bands that correspond to the phosphorylated and nonphosphorylated forms. The results obtained from both *bos1-1* and wild-type cells indicate that Sed5 is phosphorylated like the Sso and Tlg t-SNAREs (Marash and Gerst, 2001; Gurunathan *et al*., 2002).

An Aspartate Substitution at Position 317 of Sed5 Inhibits the Growth of Secretory Mutants

To explore the significance of Sed5 phosphorylation in vivo, we mutated serine-317 by substitution either with alanine to mimic the nonphosphorylated state or with aspartate to mimic the phosphorylated state. To verify that serine-317 is indeed phosphorylated, we immunoprecipitated HA-tagged Sed5 proteins from wild-type cells using anti-phosphoserine antibodies. Even though protein expression was similar, we found a large reduction in the amount of HASed5^{S317A} that could be precipitated relative to HASed5 (Figure 1F). This is consistent with the idea that serine-317 undergoes phosphorylation in vivo.

Next, we examined the growth of yeast overexpressing *SED5* or the *SED5* mutants. We found that both *SED5^{S317A}* and *SED^{5S317D}* were functional in terms of conferring growth to cells lacking the *SED5* gene (Figure 2A). The loss of Sed5 function is lethal (Hardwick and Pelham, 1992), and strains expressing a galactose-inducible form of *SED5* remained viable on glucose if they expressed native *SED5* or either mutant (Figure 2A). Similar results were observed with *sed5-1* cells, which could be rescued at restrictive temperatures (35°C) by overexpression of either mutant, although *SED5^{S317A}* expression was less effective in conferring growth (Figure 2B). Interestingly, we noted that the overexpression of *SED5* (or *SED5^{S317D}*) was inhibitory to the growth of wild-type (WT) yeast, as described previously (Hardwick and Pelham, 1992). However, this effect was not observed with *SED5^{S317A}*.

Because neither substitution inactivates Sed5, we tested their effects upon yeast defective in protein trafficking to and from the Golgi (Figure 2C). We examined their effect upon cells bearing defects in SNAREs required for ER–Golgi transport (i.e., *bos1-1*, *bet1-1*, and *sec22-2*), a COPII coat component required for anterograde transport (i.e., *sec23-2*), and a t-SNARE required for retrograde Golgi-ER transport (i.e., *ufe1-1*). We found that mutants overexpressing *SED5^{S317D}* were universally inhibited for growth at the semirestrictive temperature, whereas those expressing *SED5^{S317A}* often grew no differently than cells expressing vector alone (Figure 2C; see *bos1-1* and *ufe1-1* cells). In no case was the expression of native *SED5* or the mutants able to rescue the growth of yeast and in several cases (e.g., *bos1-1* and *ufe1-1* cells), both native *SED5* and *SED5^{S317D}* overexpression had severe inhibitory effects at normally permissive temperatures. This suggests that overexpression of the pseudophosphorylated form (*SED5^{S317D}*) as well as native *SED5*, which can undergo phosphorylation at serine-317, inhibits cell growth.

It would seem that the nonphosphorylated and pseudophosphorylated forms of Sed5 have very different effects upon cell growth. The effect upon *ufe1-1* cells by *SED5^{S317D}* was of particular interest, because Ufe1 functions in retro-

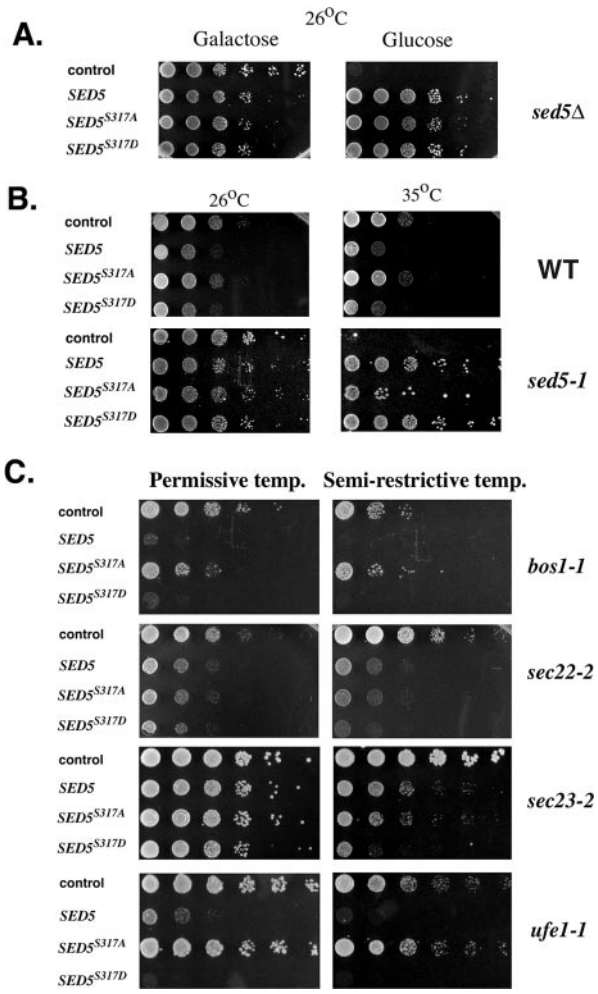

Figure 2. Effect of alanine and asparate substitutions at position 317 in Sed5 on the growth of early secretory mutants. (A) Sed5 mutants rescue *sed5*Δ cells. *sed5*Δ cells bearing a galactose-inducible *SED5* were transformed with single-copy plasmids expressing *SED5*, *SED5*^{S317A}, and *SED5*^{S317D} (plasmids pTADH-HASED5, pTADH-HASED5^{S317A}, and pTADH-HASED5^{S317D}, respectively). Cells were grown on galactose-containing medium to ensure *SED5* expression and then either shifted to glucose-containing medium overnight or maintained on galactose, before serial dilution and plating. Control, cells transformed with a control plasmid. Cells were grown on plates for >2 days. (B) Sed5 mutants rescue *sed5-1* cells. *SED5*, *SED5*^{S317A}, and *SED5*^{S317D} were expressed from multicopy plasmids (plasmids pADH-HASED5, pADH-HASED5^{S317A}, and pADH-HASED5^{S317D}, respectively) in either WT or *sed5-1* temperature-sensitive cells. Cells were grown on glucose-containing medium, diluted and plated, and grown as described in A at 26 and 35°C. The plated wild-type transformants were grown for 36 h, whereas the *sed5-1* transformants were grown for >48 h. (C) *SED5*, *SED5*^{S317A}, and *SED5*^{S317D} were expressed from multicopy plasmids in the temperature-sensitive mutants listed. Plasmids used to transform *bos1-1*, *sec22-2*, and *sec23-2* cells are as listed in B, whereas plasmids pADHU-HASED5, pADHU-HASED5^{S317A}, and pADHU-HASED5^{S317D} were used for *ufe1-1* cells. Cells were grown at permissive temperatures (26°C), diluted and plated, and grown at either permissive (26°C) or semirestrictive temperatures (32–35°C), which varied from strain to strain.

grade transport and does not cycle between compartments like Bos1 and Sec22 (Lewis and Pelham, 1996). Because *ufe1-1* cells are exquisitely sensitive to *SED5*^{S317D}, but not *SED5*^{S317A}, it suggested that phosphorylated Sed5 might affect retrograde trafficking.

An Aspartate Substitution at Position 317 of Sed5 Induces Retrograde Trafficking Defects

SED5 was identified as a multicopy suppressor of *erd2*Δ cells, which lack the HDEL receptor and thus are unable to retrieve soluble HDEL-tagged ER resident proteins to the ER (Semenza *et al.*, 1990; Hardwick and Pelham, 1992). Overproduction of Sed5 in this mutant restored retrograde trafficking back to the ER, possibly due to the enhanced vesiculation of Golgi membranes (Hardwick and Pelham, 1992). In wild-type cells, however, *SED5* overexpression causes Kar2 (Semenza *et al.*, 1990) to be secreted, perhaps due to Erd2 depletion within the Golgi (Hardwick and Pelham, 1992). Because the phosphorylation state of Sed5 affects a strain (*ufe1-1*) known to be deficient specifically in retrograde trafficking (Figure 2C), we looked for further evidence of retrograde transport defects in WT cells overproducing Sed5 or the Sed5 mutants (Figure 3). We first examined whether cells overproducing these proteins secrete Kar2, a lumenal ER resident protein secreted from yeast bearing defects in retrograde transport (Semenza *et al.*, 1990) or retention. We found that cells overexpressing either *SED5* or *SED5*^{S317D} secreted considerable amounts of Kar2 onto filters (Figure 3A, left), whereas control cells or cells overexpressing *SED5*^{S317A} secreted little or no Kar2. Because cell lysis might also account for this phenomenon, we examined the filters for the presence of cytosolic proteins (e.g., Sec1 and hexokinase). However, we found no evidence to suggest that cells overexpressing *SED5* or *SED5*^{S317D} are more labile (Weinberger and Gerst, unpublished observations). Moreover, no difference in Kar2 expression was detected in cells overexpressing *SED5* or the mutants (Weinberger and Gerst, unpublished observations). Finally, wild-type yeast expressing either *GFP-SED5* or *GFP-SED5*^{S317D} from the *SED5* locus were examined for Kar2 secretion (Figure 3A, right). Importantly, we found that cells expressing *GFP-SED5*^{S317D} secreted Kar2 to a level similar to that of *ufe1-1*. In contrast, cells expressing *GFP-SED5* (Figure 3A, right) did not secrete significant amounts of the protein. Thus, an aspartate substitution at serine-317 alone enhances Kar2 secretion. Therefore, the lack of Kar2 retention in these cells is independent of Sed5 overproduction.

Next, we followed processing of the plasma membrane GPI-anchored protein Gas1. Gas1 undergoes glycosylation upon arrival to the Golgi, which can be monitored by pulse-chase analysis and autoradiography. However, defects in retrograde transport result in an inhibition in Gas1 maturation (Sutterlin *et al.*, 1997). We found that maturation was severely inhibited in cells overexpressing *SED5* or *SED5*^{S317D} (Figure 3B), and only a small amount of mature Gas1 became visible after 45 min of chase. In addition, a low-molecular-weight form (≤50 kDa) of Gas1, which may represent a cleavage product, accumulated in a similar time-dependent manner. In contrast, mature Gas1 was readily visible within 5–10 min of chase in cells overexpressing *SED5*^{S317A} as well as in control cells. In these cells, no low-molecular-weight form was observed at ≤50 kDa. Thus, Gas1 maturation seems defective in cells overexpressing *SED5* or *SED5*^{S317D}.

The processing of the vacuolar protease carboxypeptidase Y (CPY) is used to examine anterograde transport along the secretory pathway. The p1CPY precursor is synthesized in the ER, modified in the Golgi to the larger p2CPY form, and is transported to the vacuole were it is cleaved to yield the mature form (Stevens *et al.*, 1982). We examined CPY pro-

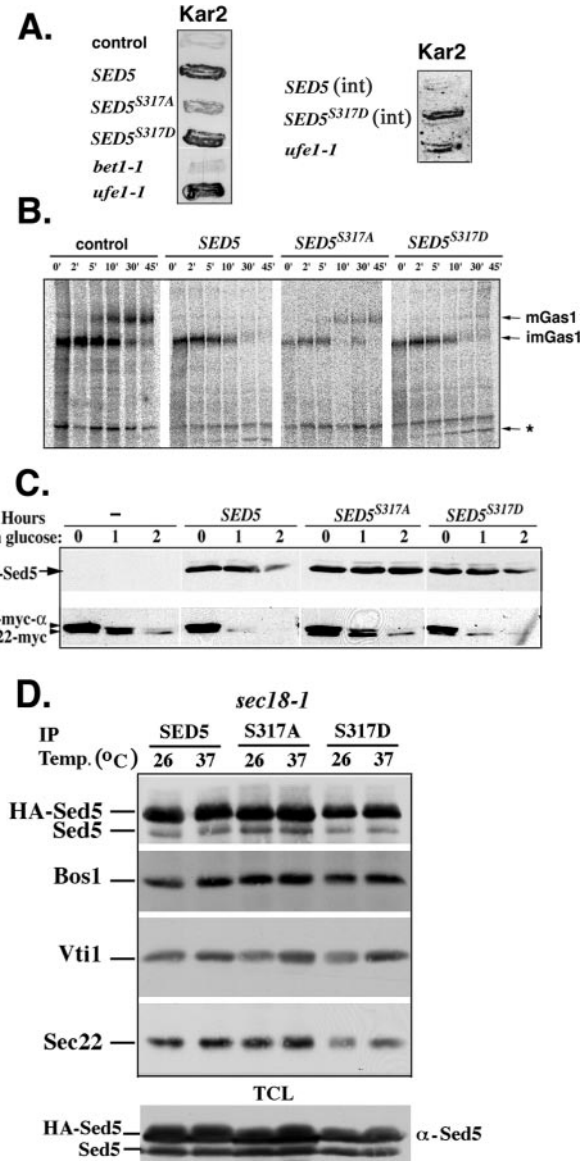

Figure 3. Overexpression of Sed5 or Sed5^{S317D} inhibits Golgi–ER retrograde transport. (A) Secretion of Kar2. Left, control (*ufe1-1* and *bet1-1*) and wild-type (SP1) cells expressing *SED5*, *SED5*^{S317A}, and *SED5*^{S317D} from multicopy plasmids (pADHU-HASED5, pADHU-HASED5^{S317A}, and pADHU-HASED5^{S317D}) were grown on synthetic medium at 26°C, replica-plated onto nitrocellulose filters (BA-S 85; Whatman Schleicher and Schuell, Dassel, Germany), and grown for 24 h. Next, cells were washed off and the filters detected for secreted Kar2, using anti-Kar2 antibodies. Right, WT (SP1) cells bearing integrated (int) forms of *GFP*-tagged *SED5* and *SED5*^{S317D} (RKY1 and RKY3 cells, respectively), and control *ufe1-1* cells were grown at 26°C, replica plated onto filters, and grown before detection with anti-Kar2 antibodies, as described above. (B) Gas1 processing. WT cells expressing *SED5*, *SED5*^{S317A}, and *SED5*^{S317D} from multicopy plasmids (pADH-HASED5, pADH-HASED5^{S317A}, and pADH-HASED5^{S317D}) were pulse-labeled with [^{35}S]methionine for 3 min, and samples were taken at the indicated time points of the chase. Gas1 was precipitated from lysates using anti-Gas1 antibodies, resolved by SDS-PAGE, and detected by autoradiography. An asterisk indicates a cleavage product at ≥50 kDa. (C) Sec22-myc-α-factor processing in cells overexpressing Sed5 mutants. Cells overexpressing *SED5*, *SED5*^{S317A}, or *SED5*^{S317D} (plasmids pADH-HASED5, pADH-HASED5^{S317A}, and pADH-HASED5^{S317D}, respectively) were transformed with a plasmid expressing the Sec22-myc-α-factor fusion under a galactose-inducible promoter. The cells were grown to log phase on galactose-containing medium and transferred to glucose-containing medium. Aliquots were removed at the indicated times, lysed, and subjected to Western analysis. Sec22-myc-α-factor (Sec22-myc-α) and Sec22-myc were detected using anti-myc antibodies, whereas Sed5 was detected using anti-HA antibodies. (D) Sed5 mutants form complexes with ER–Golgi SNAREs to the same extent as native Sed5. *sec18-1* cells expressing *HA*-tagged *SED5* (SED5), *SED5*^{S317A} (S317A) or *SED5*^{S317D} (S317D) from single copy plasmids (pLADH-HASED5, pLADH-HASED5^{S317A}, and pLADH-HASED5^{S317D}) were grown to log phase and either maintained at the permissive temperature (26°C) or shifted to the restrictive temperature (37°C) for 15 min, before processing for coimmunoprecipitation. Proteins were immunoprecipitated using anti-HA antibodies and detected in immunoblots with antibodies against Sed5, Bos1, Vti1, and Sec22. TCL, total cell lysate was detected with anti-Sed5 antibodies to demonstrate presence of HA-tagged and endogenous Sed5.

cessing in WT cells overexpressing *SED5* or the mutants by pulse-chase analysis. Unlike Gas1 processing, however, we found that CPY processing and maturation was only slightly delayed in cells expressing *SED5* or *SED5*^{S317D} (Weinberger and Gerst, unpublished observations). mCPY was observed within 30 min or less in all cell types; thus, the inhibition of transport exerted by *SED5*^{S317D} and native *SED5* overexpression seems specific to certain cargo. This may explain why cells overproducing these proteins are growth inhibited but are not inviable (Figure 2). Because at least two classes of COPII vesicles mediate ER–Golgi transport (Muniz *et al.*, 2001), it is possible that biogenesis or trafficking of the Gas1-containing class is more strongly influenced by Sed5 phosphorylation.

As anterograde transport of CPY is unaffected by *SED5* overexpression, we looked for additional retrograde transport defects. We used a Sec22-myc-α-factor (Sec22-α) reporter, which contains a Kex2 cleavage site downstream of the myc epitope (Ballensiefen *et al.*, 1998). Cells defective in retrograde transport (i.e., *sec21-1* and *ufe1-1*) fail to retrieve Sec22-α to the ER, resulting in Kex2-dependent cleavage upon reaching the *trans*-Golgi and subsequent degradation in the vacuole (Ballensiefen *et al.*, 1998). We followed the rate of disappearance of Sec22-α and its cleavage product in WT cells expressing *SED5* or the mutants (Figure 3C). Sec22-α was first expressed under the control of a *GAL* promoter overnight and then "chased" by transferring the culture to glucose-containing medium for up to 2 h. Rapid cleavage of Sec22-α was observed in cells overproducing Sed5 or Sed5^{S317D} and within 1 h even the full-length protein disappeared. However, in control cells and more so in cells expressing Sed5^{S317A}, both the full-length protein and the Kex2 cleavage product were observed for up to 2 h. Quantification revealed that 12.3 and 7.2% of the initial Sec22-α signal remained after 1 h in control and *SED5*^{S317A}-expressing cells, respectively. In contrast, cells overexpressing *SED5* or *SED5*^{S317D} showed only 0.5 and 1.1% of their initial signal. This makes it likely that Sec22-α retrieval to the ER is inhibited only in cells expressing a phosphorylatable form of Sed5. We note that Sec22-α undergoes degradation even in control cells, because its overexpression probably saturates the basal retrieval machinery (Ballensiefen *et al.*, 1998). Thus, from three independent assays we can see severe defects in retrograde transport from the Golgi to the ER, which are inflicted upon *SED5* overexpression and sustained by the phospho-mimetic form *SED5*^{S317D}. In contrast, cells expressing the nonphosphorylated form of Sed5 at position 317 have no such defects.

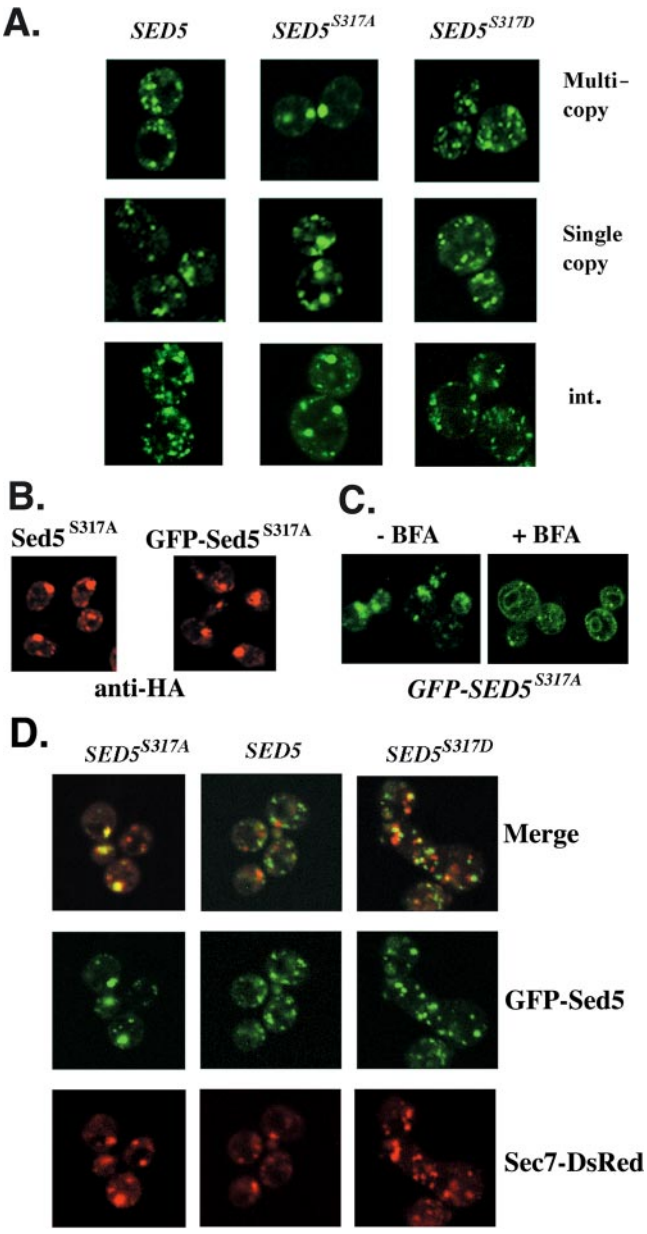

Figure 4. Sed5^{S317A} localizes to an enlarged Golgi compartment. (A) Localization of GFP-Sed5 and GFP-Sed5 mutants in WT cells. WT (SP1) cells were transformed either with multicopy (pAD54 based: pADH-HAGFPSED5, pADH-HAGFP-SED5^{S317A}, or pADH-HAGFP-SED5^{S317D}) or single-copy (pRS315 based: pLADH-HAGFPSED5, pLADH-HAGFP-SED5^{S317A}, or pLADH-HAGFP-SED5^{S317D}) plasmids that express *GFP-SED5*, *GFP-SED5^{S317A}*, or *GFP-SED5^{S317D}* or with constructs that result in the integration of either *GFP-SED5*, *GFP-SED5^{S317A}*, or *GFP-SED5^{S317D}* at the genomic *SED5* locus. The latter gene fusions are under the control of the endogenous *SED5* promoter. Cells were grown to log phase, and samples were taken for confocal microscopy. (B) Sed5^{S317A} labeling is identical to that of GFP-Sed5^{S317A}, as shown by immunofluorescence. WT cells overexpressing HA-tagged Sed5^{S317A} or HA-tagged GFP-Sed5^{S317A} were grown to log phase, fixed for immunofluorescence, and visualized using affinity-purified anti-HA antibodies and fluorescence microscopy. (C) BFA induces the dispersal of the GFP-Sed5^{S317A} labeled compartment and redistribution to the ER. *ise1*Δ cells transformed with a multicopy plasmid (pADH-HAGFPSED5^{S317A}) expressing *GFP-SED5^{S317A}* were grown to log phase, incubated either with 100 μg/ml BFA (+BFA) in medium or with medium alone (−BFA) for 15 min, and visualized by fluorescence microscopy. (D) GFP-Sed5^{S317A} colocalizes with a *trans*-Golgi marker, Sec7-RFP. WT cells containing an integrated copy of *SEC7-dsRED* (*SEC7-RFP*) were transformed with multicopy plasmids expressing *GFP-SED5*, *GFP-SED5^{S317A}*, or *GFP-SED5^{S317D}* (plasmids pADH-HAGFPSED5, pADH-HAGFP-SED5^{S317A}, or pADH-HAGFP-SED5^{S317D}). Cells were grown to log phase and visualized by fluorescence microscopy. Merge shows the overlap between GFP-Sed5 and Sec7-RFP.

Sed5^{S317A} and Sed5^{S317D} Assemble into SNARE Complexes

Because the phenotype of *SED5* overexpression is abrogated by mutating serine-317 to alanine, we speculated that the mutant might be unstable and undergo degradation. This alone could prevent the defects in retrograde transport observed upon native *SED5* overexpression. To test this, we performed pulse-chase analysis with [^{35}S]methionine and immunoprecipitated Sed5 proteins. However, we found that Sed5^{S317A} was no less stable than native Sed5 for up to 60 min and beyond (Weinberger and Gerst, unpublished observations).

An alternative explanation for the absence of an effect by Sed5^{S317A} on retrograde transport is an inability of the mutant to enter into SNARE complexes. To test this, we examined the ability of Sed5 and Sed5 mutants to interact with SNAREs in vivo by coimmunoprecipitation. We expressed HA-tagged Sed5 and the mutants from single-copy plasmids in *sec18-1* temperature-sensitive cells, which accumulate SNARE complexes at restrictive temperatures (Sogaard *et al.*, 1994). We followed the coprecipitation of SNAREs involved in ER–Golgi transport (i.e., Bos1, Sec22, and Bet1), intra-Golgi and endosomal sorting (i.e., Vti1) that are known to form complexes with Sed5 (Sogaard *et al.*, 1994; Fischer von Mollard *et al.*, 1997; Lupashin *et al.*, 1997; Tsui *et al.*, 2001; Parlati *et al.*, 2002). We found that the ability of Sed5^{S317A} to bind to Bos1, Sec22, Bet1, Ykt6, and Vti1 was similar to that of Sed5 and Sed5^{S317D} (Figure 3D; Weinberger and Gerst, unpublished observations). This implies that transport defects elicited by the alanine or aspartate substitutions are probably not mediated by changes in SNARE pairing per se.

GFP-Sed5^{S317A} Labels an Exaggerated Brefeldin A (BFA)-dissociable Compartment

Because serine-317 is proximal to the TMD of Sed5 and given that Sed5 cycles between the ER and Golgi (Wooding and Pelham, 1998), it is possible that this residue could regulate Sed5 localization. To examine this, we generated GFP-Sed5 chimeras using native Sed5 and both the alanine and aspartate substitution mutants to follow their localization in vivo by fluorescence microscopy. All three GFP-Sed5 chimeras exerted similar effects as their nonchimeric Sed5 counterparts, when expressed in *sed5-1* temperature-sensitive yeast (our unpublished data). Both GFP-Sed5 and GFP-Sed5^{S317D} had a random punctate distribution, typical of yeast Golgi markers (Figure 4A). Surprisingly, GFP-Sed5^{S317A} was distributed differently, occurring in large aggregates that are predominantly adjacent to the bud neck in wild-type cells. This was observed using both multicopy and single-copy expression plasmids as well as by genomic integration of *GFP-SED5^{S317A}* at the *SED5* locus (Figure 4A) and was reconfirmed by immunofluorescence studies using antibodies against HA-tagged Sed5^{S317A} lacking the GFP fusion (Figure 4B).

Next, we verified that GFP-Sed5^{S317A} labels Golgi membranes and is not mislocalized to other cellular compartments. We examined GFP-Sed5^{S317A} labeling in *erg6/ise1*

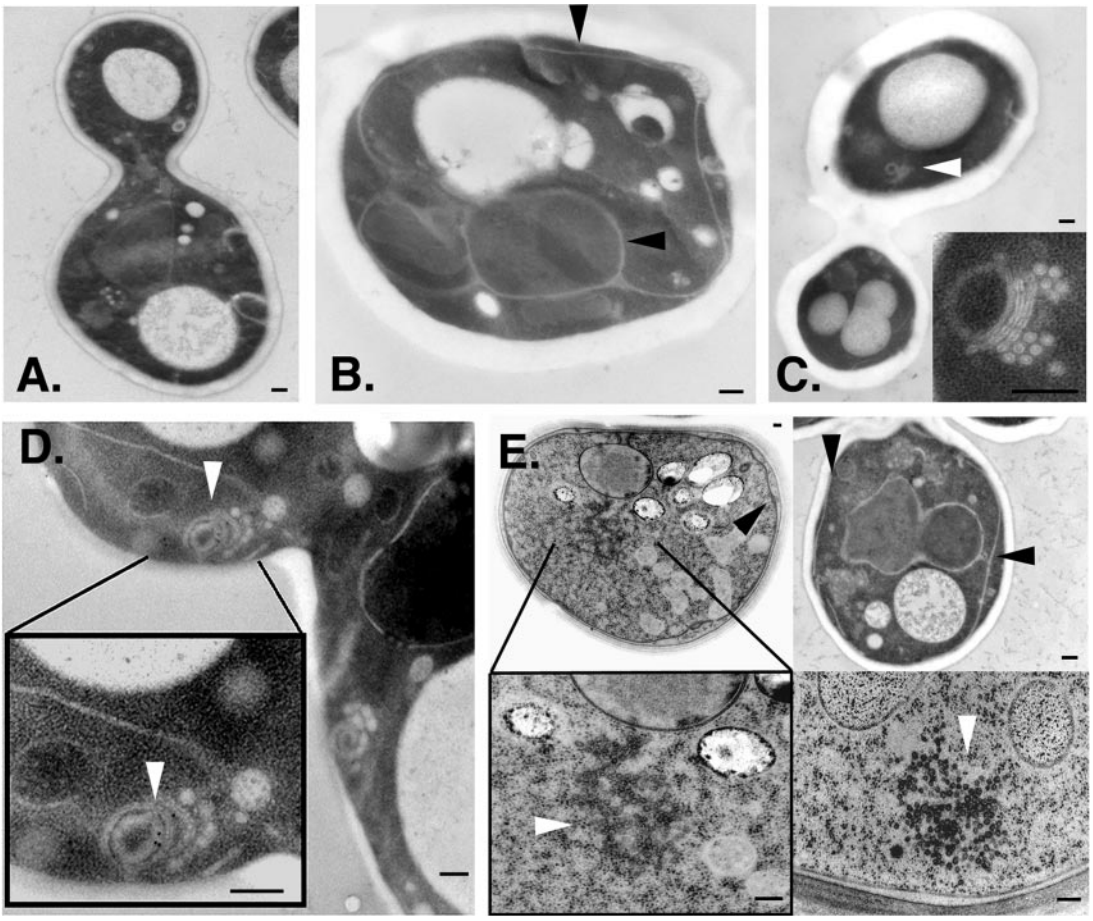

Figure 5. Sed5^{S317A} overexpression leads to an ordered Golgi stack, whereas Sed5^{S317D} overexpression induces ER elaboration and vesicle accumulation. HA-tagged *SED5*, *SED5*^{S317A}, and *SED5*^{S317D} were overexpressed from multicopy plasmids (pADH-HASED5, pADH-HASED5^{S317A}, and pADH-HASED5^{S317D}) in WT cells. Cells were harvested in log phase, fixed by HPF, and visualized by thin sectioning and electron microscopy. (A) Control WT cell. (B) Cell overexpressing *SED5*. Black arrowheads indicate elaborated ER. (C) Cell overexpressing *SED5*^{S317A}. White arrowhead indicates stacked Golgi-like structure. Inset shows example of ordered Golgi from a different cell. (D) Immunogold labeling of a cell overexpressing *SED5*^{S317A}. White arrowheads indicate ordered Golgi. Inset shows magnification of one stack; note the presence of gold particles indicating the localization of HA-tagged Sed5^{S317A} within the stack. (E) Cells overexpressing *SED5*^{S317D}. Black arrowheads indicate ER elaboration. White arrowheads indicate clusters of small vesicles. Top left, cell prepared by HPF using procedure B; bottom left, magnification of the same cell. Bottom right, example of vesicle cluster from a different cell; top right, example of cell fixed by HPF using procedure A. Bars, 0.2 μm.

cells that are permeable and sensitive to BFA, a fungal inhibitor that induces disassembly of the Golgi (Vogel *et al*., 1993; Chardin and McCormick, 1999). Surprisingly, we were unable to transform *erg6/ise1* cells with plasmids expressing *GFP-SED5* or *GFP-SED5*^{S317D} (our unpublished data) but were able to express *GFP-SED5*^{S317A}. GFP-Sed5^{S317A} labeling in this strain (Figure 4C, left) was similar to that seen in WT cells (Figure 4, A and B) and could be dispersed to the ER by treatment of the cells with BFA for 15 min (Figure 4C, right). Thus, the large compartments labeled by GFP-Sed5^{S317A} seem to represent an exaggerated Golgi apparatus.

GFP-Sed5^{S317A} *Colocalizes with a trans-Golgi Marker*

Because Sed5 is a *cis*-Golgi protein (Banfield *et al*., 1994), we examined whether GFP-Sed5^{S317A} colocalizes with late Golgi markers in the enlarged Golgi compartment. We examined colocalization with a RFP-tagged form of Sec7, a *trans*-Golgi marker (Franzusoff *et al*., 1991). In the case of GFP-Sed5 and GFP-Sed5^{S317D}, there was little colocalization observed with RFP-Sec7; however, in cells expressing Sed5^{S317A} full colocalization was evident (Figure 4D). This suggested either that the *cis*- and *trans*-markers are mixed in cells expressing Sed5^{S317A} or that the membranes bearing these fluorescent-tagged proteins are tightly juxtaposed.

GFP-Sed5^{S317A} *Expression Results in a Stacked Mammalian-like Golgi, Whereas GFP-Sed5*^{S317D} *Expression Results in Vesiculation and ER Elaboration*

To examine the intracellular morphology of cells overproducing Sed5 and the Sed5 mutants, we used electron microscopy. We overexpressed *SED5*, *SED5*^{S317D}, and *SED5*^{S317A} in WT cells and performed rapid fixation using high-pressure freezing (HPF). Interestingly, the overexpression of *SED5* and *SED5*^{S317D} led to cells having abundant and elaborated ER membranes distributed throughout the cytoplasm (Figure 5, B and E). In addition, clusters of small vesicles (40–50 nm) were readily apparent in cells overexpressing *SED5*^{S317D} (Figure 5E). Notably, similar clusters have been shown in cells depleted of Sed5 (Hardwick and Pelham, 1992).

More surprisingly, overexpression of *SED5*^{S317A} resulted in the appearance of stacked membranes reminiscent of the Golgi observed in higher eukaryotes (Figure 5, C and D). Immunogold staining of these thin sections using antibodies against the HA-tagged protein revealed the presence of Sed5^{S317A} within the stacks (Figure 5D). Thus, expression of both the nonphosphorylated and pseudophosphorylated forms of Sed5 has dramatic effects upon intracellular morphology in yeast.

Golgi Stacking Does Not Change the Distribution of Golgi Markers

To determine whether the structural changes elicited by the two forms of Sed5 alter protein distribution throughout the endomembrane system, we examined the effects of Sed5^{S317A} and Sed5^{S317D} expression by crude subcellular fractionation. We expressed HA-tagged forms of Sed5 and the mutants in WT cells and prepared two membrane fractions: a medium-speed pellet (P10) that is thought to contain the majority of the ER membranes and a high-speed pellet (P100) that includes the bulk of Golgi membranes. We then examined the distribution of various proteins, including Emp47, which localizes at steady state to the *cis*-Golgi, but recycles between the ER and Golgi (Lewis and Pelham, 1996) like Sed5 (Wooding and Pelham, 1998). We also examined the distribution of a *medial*-Golgi marker, Mnn1, and an ER marker, Dpm1. First, we noticed that native Sed5 localized to the P10 fraction, along with Dpm1, implying that the t-SNARE associates either with an ER-associated structure, perhaps the transitional ER, or that the *cis*-Golgi sedimented in this fraction (Figure 6A). Next, we found that the overproduced HA-tagged Sed5 and Sed5^{S317D} proteins were also mainly in the P10 fraction, unlike HA-tagged Sed5^{S317A}, which was evenly divided between the P10 and P100 fractions (Figure 6A). Emp47 and Mnn1 distributed primarily to the P10 fraction in cells overexpressing *SED5* and *SED5*^{S317D}, unlike in control cells or cells expressing *SED5*^{S317A} where the Golgi markers were present in both the P10 and P100 (Figure 6A). Thus, cells bearing the nonphosphorylated form of Sed5, which seem to have an ordered Golgi (Figure 5), show no alteration in the distribution of Golgi markers vis à vis control cells expressing *SED5* at native levels. In contrast, the redistribution of Golgi markers to the P10 fraction in cells overproducing either native Sed5 or its pseudophosphorylated form implies that t-SNARE phosphorylation can alter Golgi constituency.

The Nonphosphorylated Form of Sed5 Efficiently Incorporates into COPI Vesicles

Because Sed5^{S317D} overproduction inhibits retrograde transport and induces elaboration of the ER and the accumulation of vesicles, we examined its ability to enter into Golgi-derived COPI-coated vesicles thought to mediate retrograde transport. We used an in vitro Golgi budding assay (Spang and Schekman, 1998) to generate COPI vesicles in the presence of Arf1, GTP, and coatomer. COPI vesicles were generated from isolated Golgi and were fractionated by density gradient centrifugation (Figure 6B). Although Sed5^{S317A} was efficiently incorporated into vesicles along with Emp47, both Sed5 and Sed5^{S317D} were far less able to undergo packaging therein. This suggests that nonphosphorylated Sed5 may be better recruited into COPI vesicles and thus may undergo more efficient retrieval (either to the ER, within the Golgi, or both) in contrast to either the pseudophosphorylated or phosphorylatable forms of the t-SNARE.

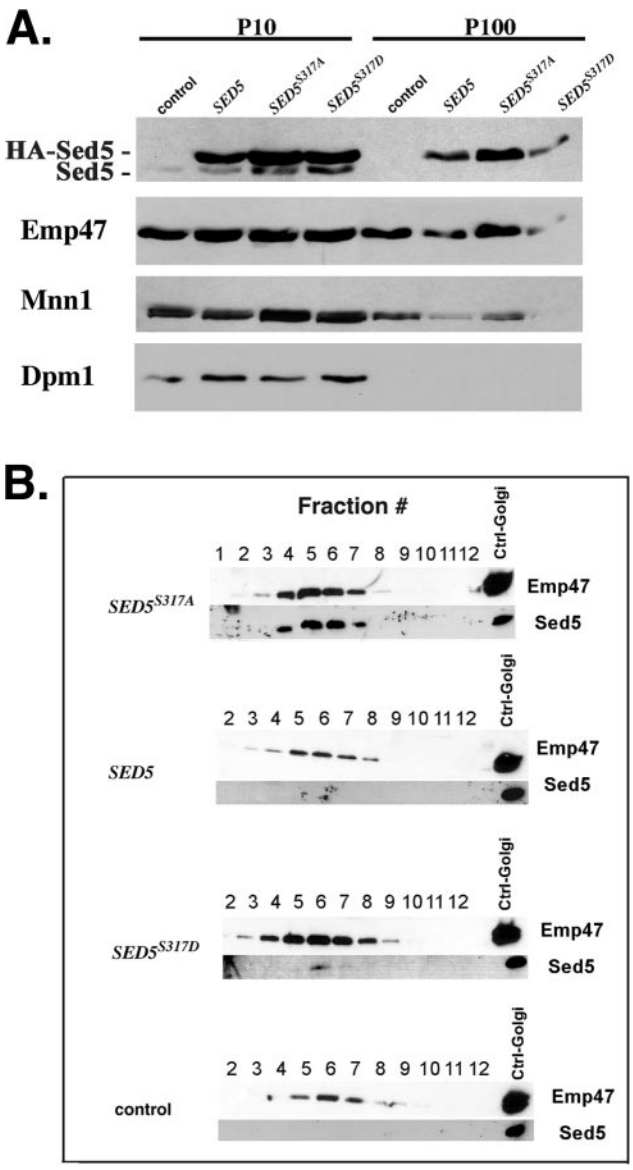

Figure 6. *SED5* and *SED5*^{S317D} overexpression induces the redistribution of Golgi markers, but they themselves are retained in the Golgi. (A) *SED5* and *SED5*^{S317D} overexpression redistributes Golgi markers. HA-tagged Sed5, Sed5^{S317A} and Sed5^{S317D} were overproduced in WT cells from multicopy plasmids (pADH-HASED5, pADH-HASED5^{S317A}, and pADH-HASED5^{S317D}, respectively). Cells were lysed in a detergent-free buffer, and the lysates were subjected to differential centrifugation to obtain a medium-speed pellet (P10) and high-speed pellet (P100) (10,000 and 100,000 $\times$ *g*, respectively). Samples of equal volume from the fractions were solubilized with SDS (1% final concentration); resolved by SDS-PAGE; and detected in blots using anti-Mnn1, anti-Emp47, anti-Dpm1, and anti-HA antibodies. (B) Sed5^{S317A} is efficiently incorporated into COPI vesicles. Cells overproducing HA-tagged Sed5, Sed5^{S317A}, and Sed5^{S317D} were grown to log phase; lysed in the absence of detergent; and a Golgi-enriched fraction prepared by differential centrifugation. The formation of COPI-coated vesicles was induced by the addition of purified coatomer, Arf1, ATP, and GTP. Vesicles were fractionated by density gradient centrifugation, and samples from the fractions were precipitated, resolved by SDS-PAGE, and detected in blots using anti-Sed5 and anti-Emp47 antibodies. Ctrl-Golgi, a sample (30 μg) of the Golgi membranes used as the source for vesicles.

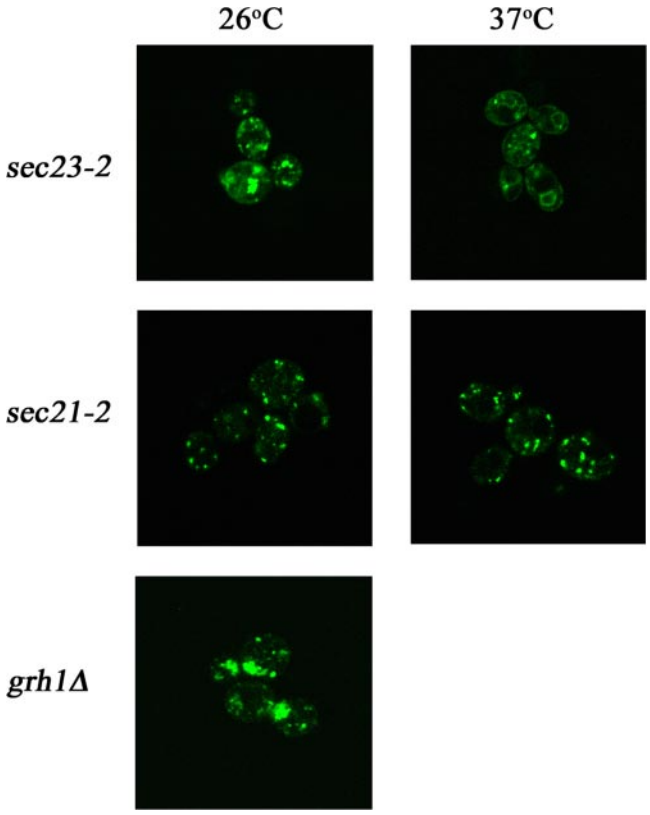

Figure 7. Retrograde Golgi–ER transport is required for formation of the enlarged Golgi compartment. Yeast strains (*sec21-2*, *sec23-2*, and *grh1*Δ) were transformed with a plasmid overexpressing *GFP-SED5*^{S317A} (pADH-HAGFPSED5^{S317A}) and examined by confocal fluorescence microscopy. Cells were examined at a temperature permissive for growth (26°C) or were shifted to the restrictive temperature (37°C), before examination.

Formation of Ordered Golgi Structures Requires Golgi-ER Retrograde Transport but Not the Yeast GRASP65 Homolog

Because Sed5^{S317A} induces the formation of an enlarged and ordered Golgi (Figures 4 and 5) and is readily able to enter into COPI vesicles unlike Sed5 and Sed5^{S317D} (Figure 6), it suggested that the ability of Sed5 to recycle, either to the ER or within the Golgi, might be an important influence upon Golgi morphology. To test this, we examined whether ordered structures could be observed in yeast defective in retrograde Golgi-ER transport. We examined the localization of GFP-Sed5^{S317A} in *sec21-2* cells, which are defective in COPI-mediated retrograde transport at restrictive temperatures (Figure 7). Interestingly, we were unable to find the enlarged Golgi aggregates typically observed in cells overproducing GFP-Sed5^{S317A} at any temperature (Figure 4). Instead, the labeling of GFP-Sed5^{S317A} in *sec21-2* cells (Figure 7) was similar to that observed for GFP-Sed5 in wild-type cells (Figure 4); 92% of cells (n = 100) expressing GFP-Sed5^{S317A} did not show Golgi aggregates. In contrast, the enlarged Golgi puncta were readily observed in *sec23-2* cells, which bear defects in anterograde ER–Golgi transport, at permissive temperatures, whereas labeling of the ER was observed at the restrictive temperature, as expected (Figure 7). Thus, Sed5 recycling is likely to be important for the formation of ordered Golgi structures.

Next, we examined whether the yeast orthologue of GRASP65, a protein known to function in the postmitotic reassembly of the Golgi in mammalian cells (Shorter and Warren, 2002), is necessary for formation of an ordered Golgi. We overproduced GFP-Sed5^{S317A} in cells lacking *GRH1*, but we found no obvious defects in formation of the fluorescent puncta (Figure 7). This suggests that this orthologue is not necessary for Golgi stacking per se

DISCUSSION

Because t-SNARE phosphorylation and dephosphorylation seem to play a significant role in regulation of the exo- and endocytic processes (Weinberger and Gerst, 2004), we examined whether ER–Golgi transport is controlled in a similar manner. Here, we show that an essential Golgi t-SNARE, Sed5, is a phosphoprotein and that phosphorylation controls the morphology and apparent functioning of the Golgi apparatus. Sed5 overproduction inhibits the growth of yeast (Hardwick and Pelham, 1992; Figure 2), which is recapitulated in an even stronger manner by the replacement of a conserved serine residue (serine-317) with aspartate (Figure 2, B and C). In contrast, this phenotype is abrogated by introduction of an alanine residue in place of the relevant serine (Figure 2, B and C). Thus, both phosphorylation and dephosphorylation of this residue seem to play a critical role in Sed5 functioning.

Although both the aspartate and alanine substitutions confer growth to yeast lacking a functional Sed5 (Figure 2), the aspartate-317 substitution results in a marked decrease in the growth of *bos1-1*, *sec23-2*, and *ufe1-1* cells (Figure 2C). However, only *ufe1-1* cells are specifically defective in Golgi–ER retrograde transport (Lewis and Pelham, 1996). Other postulated retrograde transport defects, such as Kar2 secretion, an inhibition of Gas1 processing, and the pronounced degradation of a Sec22-α-factor chimeric protein, were all observed in wild-type cells expressing *SED5*^{S317D} (Figure 3). Similar results were obtained with overproduced native Sed5, which can undergo phosphorylation, but not with the nonphosphorylatable alanine substitution at position-317 (Figure 3). Importantly, these transport defects are not consistent with a general deficiency in protein export from either the ER or the Golgi. For example, Kar2 and Sec22-α-factor either reach post-Golgi compartments or are exported (Figure 3, A and C). Next, GFP-Sed5 and GFP-Sed5^{S317D} give punctate labeling that is typical of the Golgi and not the ER (Figure 4A), indicating that they can exit early compartments. Finally, CPY maturation is not blocked in cells overexpressing Sed5^{S317D} (Weinberger and Gerst, unpublished observations). Although Gas1 maturation does seem inhibited (Figure 3B), this export defect has also been shown in cells defective in retrograde transport (Sutterlin *et al*., 1997). Thus, our observations implicate serine-317 phosphorylation as a potential regulator of Golgi–ER retrograde transport.

Supportive of this view is electron microscopy data showing ER elaboration and the accumulation of small clustered transport vesicles in cells expressing the aspartate-317 substitution (Figure 5E). Because a similar phenotype was observed in cells lacking Sed5 (Hardwick and Pelham, 1992), it suggests that constitutive phosphorylation of serine-317 can have an effect analogous to decreased Sed5 function in some assays. However, the overexpression of native *SED5* also inhibited cell growth (Figure 2C) and induced both retrograde sorting defects and ER elaboration (Figures 3, A–C, and 5) as well as *SED5*^{S317D}, but it could not induce vesicle accumulation (Figure 5). Thus, although the phospho-mi-

metic mutant is clearly functional (Figures 2A and 3D), it can exert effects unlike that of the native t-SNARE. Thus, the effects of *SED5* and *SED5*^{S317D} overexpression are comparable but not necessarily identical. This may explain why the aspartate substitution mutant is more potent in some assays (Figures 2C, 3A, and 5). Although the mechanism for vesicle accumulation in cells expressing *SED5*^{S317D} is unclear, it suggests defects in either the fusion of Golgi-derived COPI vesicles with the ER or COPII vesicles with the Golgi. The former possibility is more likely, because defects in retrograde transport invariably block the budding of ER-derived transport vesicles and lead to the accumulation of ER membrane. More work will be required to verify the nature of these vesicles.

If the vesicles observed in *SED5*^{S317D}-expressing cells are indeed retrograde transport vesicles, why should they be less able to fuse? The answer may lie with the fact that Sed5^{S317D} and phosphorylatable native Sed5 inefficiently incorporate into Golgi-derived COPI vesicles in vitro (Figure 6B). Perhaps Sed5 is required for *trans*-SNARE pairing with ER resident SNAREs (i.e., Ufe1, Sec20, and Sec22) to form a retrograde fusion complex. Alternatively, it may be needed to chaperone cycling SNAREs (i.e., Bos1, Bet1, and Sec22) or other factors back to the ER. In either case, it would explain why Sed5 cycles between compartments (Wooding and Pelham, 1998). Another possibility is that the phosphorylated form of Sed5 binds to Arf GTPases less well, thus decreasing the formation of retrograde transport vesicles. However, this possibility is less likely, given that such vesicles can be formed in the presence of Sed5^{S317D} (Figure 6B) and that in vitro binding studies with the Sed5 mutants and recombinant myristoylated Arf1 showed no difference in Arf binding (Spang, unpublished observations). Fractionation experiments suggest that the constituency of the Golgi may change upon *SED5* or *SED5* ^{S317D} overexpression and that a redistribution of Golgi markers to a heavier ER-enriched fraction occurs (Figure 6A). Ironically, this happens even though Sed5^{S317D} (or native Sed5) does not efficiently enter into COPI vesicles in vitro like Sed5^{S317A} (Figure 6B). Because GFP-Sed5^{S317D} does not yield ER-like labeling (Figure 4D), it is unlikely that it associates with ER membranes and presumably is associated with the early Golgi. More work will be required to understand the connection between altered Sed5 recruitment into COPI vesicles and the redistribution of the Golgi markers.

Our other major observation is that the nonphosphorylated form of Sed5, Sed5^{S317A}, results in the accumulation of an ordered Golgi reminiscent of the stacked apparatus found in higher eukaryotes (Figure 5, C and D). Although cells expressing Sed5^{S317A} show no defects in protein trafficking or growth (Figure 2); nonetheless, the dispersed Golgi typical of *S. cerevisiae* seems absent. Thus, formation of an ordered Golgi from a disordered state seems to have no debilitating effects upon the growth of yeast per se. Indeed, other yeast, such as *Pichia pastoris*, favor an ordered state (Glick, 1996). The differences between these yeast are thought to result from the number of sites available for COPII vesicle budding, which bud from fixed sites in *P. pastoris* and throughout the ER in *S. cerevisiae* (Rossanese *et al*., 1999). This may be responsible for the formation of either polarized or scattered transitional ER, respectively, which eventually coalesce to form the Golgi (Rossanese *et al*., 1999). Our results imply that a lack of phosphorylation at position 317 of Sed5 induces an ordered state of the Golgi (Figure 5, C and D, and model in Figure 8). In contrast, pseudophosphorylation induces a dispersed state, if the vesicles that accumulate therein are COPI vesicles (Figure 5E and model in Figure 8). Thus, a dynamic cycle of t-SNARE phosphorylation and dephosphorylation may be necessary for the Golgi to maintain structural integrity even in *S. cerevisiae*. Changes in the ability of Sed5 to cycle (via phosphorylative control) can also be expected to play a role in the de novo formation of the early Golgi from the transitional ER (Rossanese *et al*., 2001).

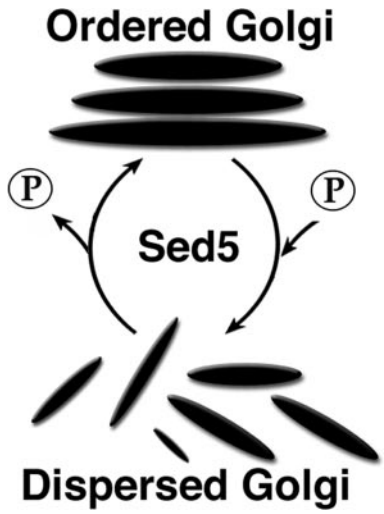

Figure 8. Model for Golgi morphology as a consequence of Sed5 phosphorylation. Sed5 in its nonphosphorylated (at position 317) state results in a stacked mammalian-like Golgi structure (Ordered Golgi). In contrast, upon phosphorylation at position 317 Sed5 induces the dispersal of Golgi markers, the accumulation of transport vesicles and ER, and inhibits cell growth (Dispersed Golgi). Thus, Golgi structure may alternate between structured and unstructured states as a consequence of t-SNARE phosphorylation.

How can the phosphorylation state of a SNARE influence organelle integrity so dramatically? One clue is that Sed5 acts upon multiple Golgi transport pathways, including anterograde transport to the *cis*-Golgi (using the Bos1, Bet1, and Sec22 SNAREs), intra-Golgi transport (using the Sft1, Got1, and Ykt6 SNAREs) as well as endosome-to-Golgi transport (using Tlg1, Vti1, and Gos1 SNAREs). Therefore, Sed5 localization must be controlled such that it maintains a steady-state distribution to the *cis*-Golgi (Hardwick and Pelham, 1992; Wooding and Pelham, 1998), but nevertheless can transverse the cisternae to interact productively with its other SNARE partners or to be retrieved to the ER.

We propose that Sed5 transport and retrieval through the Golgi is regulated by its phosphorylation state. The alanine substitution mutant, whose expression results in an ordered Golgi (Figures 4 and 5), and that efficiently incorporates into COPI vesicles (Figure 6B), implies that enhanced Sed5 retrieval back through the cisternae might induce stacking. This is supported by studies in *sec21-2* cells, which are defective in retrograde transport, and do not allow for formation of ordered Golgi structures (Figure 7). However, we do note that Sed5^{S317A} colocalizes with Sec7, a *trans*-Golgi marker, implying a steady-state presence in the *trans*-Golgi (Figure 4D). This, as well, might account for the ordering phenomenon and therefore requires further study. It is noteworthy to add that stacking could also result from the alanine mutant independently of its enhanced packaging into COPI vesicles or retrograde transport. In contrast to Sed5^{S317A}, the aspartate substitution mutant, which is inefficiently incorporated into COPI vesicles (Figure 6B) and whose expression results in ER elaboration and vesicle ac-

cumulation (Figure 5), may reside too efficiently in the *cis*-compartment such that it inhibits retrograde transport events and therefore cell growth (Figures 2 and 3). The mechanism for Sed5 retention is also not well understood, but previous studies suggested that it is determined by the cytoplasmic domain and not by the TMD (Banfield *et al*., 1994), in contrast to other SNAREs such as Snc1 (Lewis *et al*., 2000). Serine-317, which is adjacent to the TMD, is therefore a strong candidate for a Sed5 Golgi retention signal upon phosphorylation.

Finally, we note that stacked Golgi-like structures have been observed in other secretory mutants of *S. cerevisiae*; however, these are seen at temperatures where Golgi export is blocked (i.e., in *sec7*, *sec14*, and *ypt31Δ ypt32-1* cells; Novick *et al*., 1981; Franzusoff *et al*., 1991; Jedd *et al*., 1997), whereas the ordered structures observed in Sed5^{S317A}-expressing cells occur under conditions conducive for growth (Figures 2 and 5). Thus, ordering per se has no deleterious effects although the alanine mutant is not as effective for the rescue of *sed5-1* cells (Figure 2B). An ordered organization of the Golgi, as seen in higher eukaryotes, may prove useful where ER exit sites are more tightly controlled, leading to the polarized accumulation of transitional ER (and subsequent Golgi coalescence). This may be of particular importance as cell size increases, allowing for more efficient transport between cisternae as well as to target compartments. The fact that a t-SNARE mutation can bring about such morphological changes suggests that a controlled mechanism for ordering and dispersal exists. This is likely to be important for Golgi assembly and disassembly during the mitotic cell cycle in higher eukaryotes, which also involves cycles of protein phosphorylation and dephosphorylation. In particular, the functioning of several Golgi structural proteins (i.e., GM130, GRASP65, and p115) during mitosis has been shown to be modulated by phosphorylation and in a manner that correlates with Golgi fragmentation and dispersal (reviewed in Rossanese and Glick, 2001; Shorter and Warren, 2002).

ACKNOWLEDGMENTS

We thank D. Banfield, C. Barlowe, S. Emr, G. Fischer von Mollard, B. Glick, M. Lewis, P. Novick, H. Pelham, H. Riezman, R. Schekman, H-D. Schmidt, G. Warren, and M. Wigler for the generous gifts of reagents. We also gratefully thank V. Shindler (Weizmann Institute of Science) and H. Schwarz (Max-Planck-Institute for Developmental Biology, Tübingen, Germany) for electron microscopy work. This work was supported by grants to J.E.G. from the Israel Science Foundation (374/02-1) and the M. D. Moross Institute for Cancer Research; A. S. from the Deutsche Forschungsgemeinshaft and Max Planck Gesellschaft; and to both J.E.G and A. S. by the Minna James Heineman/Minerva Foundation, Germany. J.E.G. holds the Henry Kaplan Chair in Cancer Research. A. S. is a European Molecular Biology Organization Young Investigator.

REFERENCES

Ballensiefen, W., Ossipov, D., and Schmitt, H. D. (1998). Recycling of the yeast v-SNARE Sec22p involves COPI-proteins and the ER transmembrane proteins Ufe1p and Sec20p. J. Cell Sci. *111*, 1507–1520.

Banfield, D. K., Lewis, M. J., Rabouille, C., Warren, G., and Pelham, H. R. (1994). Localization of Sed5, a putative vesicle targeting molecule, to the *cis*-Golgi network involves both its transmembrane and cytoplasmic domains. J. Cell Biol. *127*, 357–371.

Chardin, P., and McCormick, F. (1999). Brefeldin A: the advantage of being uncompetitive. Cell *97*, 153–155.

Chen, Y. A., and Scheller, R. H. (2001). SNARE-mediated membrane fusion. Nat. Rev. Mol. Cell. Biol. *2*, 98–106.

Couve, A., Protopopov, V., and Gerst, J. E. (1995). Yeast synaptobrevin homologs are modified post-translationally by the addition of palmitate. Proc. Natl. Acad. Sci. USA *92*, 5987–5991.

Farquhar, M. G., and Palade, G. E. (1998). The Golgi apparatus: 100 years of progress and controversy. Trends Cell Biol. *8*, 2–10.

Fischer von Mollard, G., Nothwehr, S. F., and Stevens, T. H. (1997). The yeast v-SNARE Vti1p mediates two vesicle transport pathways through interactions with the t-SNAREs Sed5p and Pep12p. J. Cell Biol. *137*, 1511–1524.

Franzusoff, A., Redding, K., Crosby, J., Fuller, R. S., and Schekman, R. (1991). Localization of components involved in protein transport and processing through the yeast Golgi apparatus. J. Cell Biol. *112*, 27–37.

Glick, B. S. (1996). Cell biology: alternatives to baker's yeast. Curr. Biol. *6*, 1570–1572.

Gurunathan, S., Marash, M., Weinberger, A., and Gerst, J. E. (2002). t-SNARE phosphorylation regulates endocytosis in yeast. Mol. Biol. Cell *13*, 1594–1607.

Hardwick, K. G., and Pelham, H. R. (1992). SED5 encodes a 39-kD integral membrane protein required for vesicular transport between the ER and the Golgi complex. J. Cell Biol. *119*, 513–521.

Jedd, G., Mulholland, J., and Segev, N. (1997). Two new Ypt GTPases are required for exit from the yeast trans-Golgi compartment. J. Cell Biol. *137*, 563–580.

Lewis, M. J., Nichols, B. J., Prescianotto-Baschong, C., Riezman, H., and Pelham, H. R. (2000). Specific retrieval of the exocytic SNARE Snc1p from early yeast endosomes. Mol. Biol. Cell *11*, 23–38.

Lewis, M. J., and Pelham, H. R. (1996). SNARE-mediated retrograde traffic from the Golgi complex to the endoplasmic reticulum. Cell *85*, 205–215.

Longtine, M. S., McKenzie, A., Demarini, D., Shah, N. G., Wach, A., Brachat, A., Philippsen, P., and Pringle, J. R. (1998). Additional modules for versatile and economical PCR-based gene deletion and modification in *Saccharomyces cerevisiae*. Yeast *14*, 953–961.

Lupashin, V. V., Pokrovskaya, I. D., McNew, J. A., and Waters, M. G. (1997). Characterization of a novel yeast SNARE protein implicated in Golgi retrograde traffic. Mol. Biol. Cell *8*, 2659–2676.

Lustgarten, V., and Gerst, J. E. (1999). Yeast *VSM1* encodes a v-SNARE binding protein that may act as a negative regulator of constitutive exocytosis. Mol. Cell. Biol. *19*, 4480–4494.

Marash, M., and Gerst, J. E. (2001). t-SNARE dephosphorylation promotes SNARE assembly and exocytosis in yeast. EMBO J. *20*, 411–421.

Marash, M., and Gerst, J. E. (2003). Phosphorylation of the autoinhibitory domain of the Sso t-SNAREs promotes binding of the Vsm1 SNARE regulator in yeast. Mol. Biol. Cell *14*, 3114–3125.

Muniz, M., Morsomme, P., and Riezman, H. (2001). Protein sorting upon exit from the endoplasmic reticulum. Cell *104*, 313–320.

Nichols, B. J., and Pelham, H. R. (1998). SNAREs and membrane fusion in the Golgi apparatus. Biochim. Biophys. Acta *1404*, 9–31.

Novick, P., Ferro, S., and Schekman, R. (1981). Order of events in the yeast secretory pathway. Cell *25*, 461–469.

Parlati, F., Varlamov, O., Paz, K., McNew, J. A., Hurtado, D., Sollner, T. H., and Rothman, J. E. (2002). Distinct SNARE complexes mediating membrane fusion in Golgi transport based on combinatorial specificity. Proc. Natl. Acad. Sci. USA *99*, 5424–5429.

Pelham, H. R. (1998). Getting through the Golgi complex. Trends Cell Biol. *8*, 45–49.

Pelham, H. R. (1999). SNAREs and the secretory pathway-lessons from yeast. Exp. Cell Res. *247*, 1–8.

Pelham, H. R., and Rothman, J. E. (2000). The debate about transport in the Golgi-two sides of the same coin? Cell *102*, 713–719.

Rossanese, O. W., Soderholm, J., Bevis, J., Sears, I. B., O'Connor, J., Williamson, E. K., and Glick, B. S. (1999). Golgi structure correlates with transitional endoplasmic reticulum organization in *Pichia pastoris* and *Saccharomyces cerevisiae*. J. Cell Biol. *145*, 69–81.

Rossanese, O. W., and Glick, B. S. (2001). Deconstructing the Golgi. Traffic *2*, 589–596.

Rossanese, O. W., Reinke, C. A., Bevis, B. J., Hammond, A. T., Sears, I. B., O'Connor, J., and Glick, B. S. (2001). A role for actin, Cdc1p, and Myo2p in the inheritance of late Golgi elements in *Saccharomyces cerevisiae*. J. Cell Biol. *153*, 47–62.

Semenza, J. C., Hardwick, K. G., Dean, N., and Pelham, H. R. (1990). ERD2, a yeast gene required for the receptor-mediated retrieval of luminal ER proteins from the secretory pathway. Cell *61*, 1349–1357.

Shorter, J., and Warren, G. (2002). Golgi architecture and inheritance. Annu. Rev. Cell Dev. Biol. *18*, 379–420.

Sogaard, M., Tani, K., Ye, R. R., Geromanos, S., Tempst, P., Kirchhausen, T., Rothman, J. E., and Sollner, T. (1994). A Rab protein is required for the assembly of SNARE complexes in the docking of transport vesicles. Cell *78*, 937–948.

Spang, A., and Schekman, R. (1998). Reconstitution of retrograde transport from the Golgi to the ER *in vitro*. J. Cell Biol. *143*, 589–599.

Stevens, T., Esmon, B., and Schekman, R. (1982). Early stages in the yeast secretory pathway are required for transport of carboxypeptidase Y to the vacuole. Cell *30*, 439–448.

Sutterlin, C., Doering, T. L., Schimmoller, F., Schroder, S., and Riezman, H. (1997). Specific requirements for the ER to Golgi transport of GPI-anchored proteins in yeast. J. Cell Sci. *110*, 2703–2714.

Tsui, M. M., Tai, W. C., and Banfield, D. K. (2001). Selective formation of Sed5p-containing SNARE complexes is mediated by combinatorial binding interactions. Mol. Biol. Cell *12*, 521–538.

Vogel, J. P., Lee, J. N., Kirsch, D. R., Rose, M. D., and Sztu, E. S. (1993). Brefeldin A causes a defect in secretion in *Saccharomyces cerevisiae*. J. Biol. Chem. *268*, 3040–3043.

Weinberger, A., and Gerst, J. E. (2004). Regulation of SNARE assembly by protein phosphorylation. Top. Curr. Genet. *10*, 145–170.

Wooding, S., and Pelham, H .R. (1998). The dynamics of Golgi protein traffic visualized in living yeast cells. Mol. Biol. Cell *9*, 2667–2680.

Yamaguchi, T., Dulubova, I., Min, S. W., Chen, X., Rizo, J., and Sudhof, T. C. (2002). Sly1 Binds to Golgi and ER syntaxins via a conserved N-terminal peptide motif. Dev. Cell *2*, 295–305.